# Galvanic Cell Type Sensor for Soil Moisture Analysis

Pramod Gaikwad,[†] Mruthyunjayachari Chattanahalli Devendrachari,[†] Ravikumar Thimmappa,[†] Bhuneshwar Paswan,[†] Alagar Raja Kottaichamy,[†] Harish Makri Nimbegondi Kotresh,[‡] and Musthafa Ottakam Thotiyl*,[†]

[†]Indian Institute of Science Education and Research (IISER) Pune, Dr. Homi Bhabha Road, Pashan, Pune 411008, India
[‡]Department of Chemistry, Acharya Institute of Technology, Soldevanahalli, Bangalore 560107, India

S *Supporting Information*

ABSTRACT: Here we report the first potentiometric sensor for soil moisture analysis by bringing in the concept of Galvanic cells wherein the redox energies of Al and conducting polyaniline are exploited to design a battery type sensor. The sensor consists of only simple architectural components, and as such they are inexpensive and lightweight, making it suitable for on-site analysis. The sensing mechanism is proved to be identical to a battery type discharge reaction wherein polyaniline redox energy changes from the conducting to the nonconducting state with a resulting voltage shift in the presence of soil moisture. Unlike the state of the art soil moisture sensors, a signal derived from the proposed moisture sensor is probe size independent, as it is potentiometric in nature and, hence, can be fabricated in any shape or size and can provide a consistent output signal under the strong aberration conditions often encountered in soil moisture analysis. The sensor is regenerable by treating with 1 M HCl and can be used for multiple analysis with little read out hysteresis. Further, a portable sensor is fabricated which can provide warning signals to the end user when the moisture levels in the soil go below critically low levels, thereby functioning as a smart device. As the sensor is inexpensive, portable, and potentiometric, it opens up avenues for developing effective and energy efficient irrigation strategies, understanding the heat and water transfer at the atmosphere−land interface, understanding soil mechanics, forecasting the risk of natural calamities, and so on.
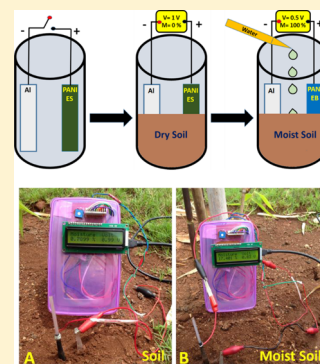
oil moisture content (SMC) is a definitive parameter in the ecological water cycle, meteorology, agriculture, forestry, soil mechanics, etc., and it is a deciding factor in many hydrological, biological, and biogeochemical actions.[1−5] SMC influences the weather and climate of our ecosystem by influencing the land surface and atmospheric interactions and thereby regulating the precipitation and evapotranspiration, and it provides a link between water, energy, and carbon cycles.[5−8] In agriculture, preserving the appropriate SMC is critically important because it can influence the seed sprouting, soil organic component's disintegration, nutrient transfer, and root respiration. Efficient water management practices are therefore essential for sustainable and fruitful agriculture in times of high energy and water costs.[9] All these calls for continuous soil moisture monitoring and implementation of such technologies can help in effective irrigation strategies, forecasting the risk of natural calamities, understanding of heat and water transfer at the atmosphere−land interface, and so on.

The widely used direct method for soil moisture analysis is the gravimetric method and is often considered as destructive and time-consuming and, hence, not worthy for on-site analysis.[9−11] Though the indirect neutron moderation method usually provides the user with robust and accurate data, it suffers from safety issues apart from expensive instrumentation and the requirement of skilled personnel.[12,13] The dielectric and electromagnetic methods commonly employed for soil moisture analysis require complex electronic circuits and thus are relatively expensive.[14] One common problem encountered in many of these indirect methods is the dependence of the probe size on the output signal. For example, in the capacitance sensor, the probe is subjected to an excitation frequency and the moisture dependent response often varies with the areal parameters of the probe.[15]

Here we have successfully developed a simple, inexpensive, and portable soil moisture sensor by bringing in the concept of Galvanic cells. The developed Galvanic type sensor is the first of its kind in soil moisture analysis and does not require an external power input to function (power input is required only for the microcontroller and the display), unlike the state of the art soil moisture sensors. For example, the dielectric and electromagnetic sensing probes require a voltage input to generate the sensing signals at the probe, which is not the case for the sensing probes we developed, as it is potentiometric in nature. The formulated sensor is lightweight (∼100 g) and requires only a simple voltmeter to measure the moisture level accurately, and hence, it is ideally suited for field analysis for evaluating the spatial and temporal variations of moisture levels in an area. It is very important to note that, unlike the state of

the art moisture sensors, the signal derived from the proposed moisture sensor is probe size independent, as it is potentiometric in nature and hence can be fabricated in any shape or size and can provide consistent output under strongly aberration conditions commonly encountered in soil moisture analysis.

■ EXPERIMENTAL PROCEDURES

Materials and Methods. HCl, H_2SO_4, Al foil, ammonium per sulfate, aniline, and ethanol were of analytical grade and were procured from Alfa Aesar, India. Aniline was distilled before use. Whatman filter paper 40 (SDFCL) was used for PANI deposition.

Preparation of Conducting PANI Embedded Filter Paper. Commercially available Whatman 40 filter paper with dimension 5 cm diameter was taken in a Petri dish. A stock solution of anilinium chloride solution was prepared by mixing 0.3063 g of aniline with 5 mL of 2 M HCl solution in distilled water. The stock solution was uniformly distributed on one side of the filter paper and allowed to be soaked for 2−3 min. Then the solution 1.88 g of ammonium per sulfate was added drop by drop and the filter paper was allowed to dry. The filter paper turned to light green in 20 min and dark green in about 40 min. The filter paper was washed thoroughly with water and dried again.

The photograph of the synthesized PANI paper is shown in Figure S1 and it showed dark green colored deposit on the paper surface indicating the formation of conducting emeraldine salt (ES) form of PANI.

Fabrication of Moisture Sensing Probes. Conducting PANI was coated on filter paper by oxidative polymerization as explained above. Five ×5 cm of PANI paper and 5 × 5 cm Al foil were wrapped on Teflon (10 cm in length) rods. The probe end was insulated using Teflon tape and at other end was given the electrical connection which was further wrapped with Teflon tapes to insulate the connecting wires.

Characterization. UV−vis spectroscopy (PerkinElmer Lambda 950) was carried out in a quartz cuvette. % transmittance of PANI before and after use for soil moisture analysis was measured in the UV−vis region. FTIR was carried out for the PANI electrodes before and after soil moisture analysis using a Bruker Alpha ATR-FTIR. XRD of samples were measured using a Bruker D8 Advance diffractometer. XPS spectrum of PANI was recorded using Thermo K-Alpha (Thermo Scientific, East Grinstead, UK) using a monochromatic Al Kα source at 100 W. C (1s) signal was used to correct the spectral shifts and a Shirley background subtraction was employed for background correction. Galvanostatic discharge measurements were carried out in two electrode configuration at a specific discharge current of 500 μA in 0.1 M H_2SO_4 medium using a CHI 660B electrochemical workstation. Impedance spectra were acquired in the range 100 kHz to 10 mHz at 0 V vs open circuit voltage (OCV). The cyclic voltammogram of PANI supported on glassy carbon electrode was acquired using a three-electrode configuration with a Pt counter electrode and a saturated calomel reference electrode.

Device Fabrication and Calibration. We have fabricated a moisture sensing device based on Al-PANI Galvanic cell. The block diagram for the total device is presented in Figure S2A, and as shown the first block is the sensor. The electronic circuitry is shown in the Figure S2B. Output of moisture sensor was in the form of voltage. Changes in moisture levels at the input of the sensor can be simultaneously read as voltage at the

output of the sensor. This output was in the form of analog data, so it became essential to convert it into digital form because the microcontroller reads only digital data. For this reason output voltage was given to analog to digital converter (ADC, 10 bit). ADC is an electronic device which converts analog data into digital data. In the circuitry in Figure S2B, ADC is not seen because AVR (Atmega-32) microcontroller has inbuilt ADC. Microcontroller is an electronic device that includes microprocessor, memory and I/O (input/output) device on a single chip using the VLSI technology. A microcontroller is a true computer on a chip. The program was written in win AVR software as per the calibration. This was tested on a simulation tool (Proteus) before making the hardware and after obtaining successful results, the hardware was fabricated. Orcad software was used for drawing the circuit layouts. After the completion of the hardware and software parts, the software (program) was burnt into the microcontroller chip. The display system was 16*2 alphanumeric parallel liquid crystal display. Five Volts power supply unit provided power to all subunits such as microcontroller, display and ADC. The architectural components and the cell arrangements are shown in Scheme 1 and it consists of an Al

Scheme 1. Schematic Explaining the Cell Arrangements and the Sensing Mechanism at the Sensing Probes during Soil Moisture Analysis[a]
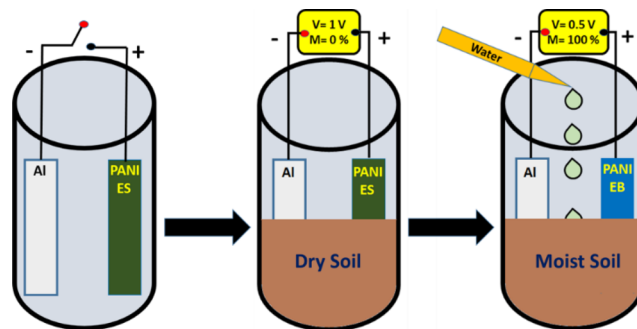
[a]"M" in the display panel stands for the soil moisture content. ES and EB stand for conducting and nonconducting forms of polyaniline (PANI).

anode and a conducting PANI (ES) cathode. In the presence of soil moisture the voltage difference between the sensing electrodes drop which is nearly linear in its response to the soil moisture content. The complete set up of the device with an alphanumeric liquid crystal display is shown in Figure 1 along with sensing probes.
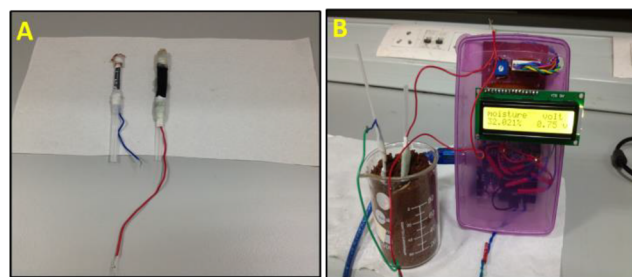

Figure 1. Architectural components of the moisture sensor: (A) Al and PANI sensing electrodes and (B) the complete soil moisture sensing device with alphanumeric liquid crystal display.

Calibration of moisture sensor was done by measuring the potential difference between the Al and PANI electrodes inserted in dry soil before and after quantitative addition of water (pH = 7) as shown in Scheme 1. Before starting the calibration, soil was dried completely using a vacuum oven. The fabricated sensing probes were inserted in to the soil in such a manner that the distance between the two probes were less than 1 cm and determined the potential difference between the electrodes as a function of moisture levels, and then obtained the calibration plot of potential vs % moisture. Recorded potential for dry soil corresponded to 0% moisture. For each moisture level, 5−10 min waiting period was employed to get a stable reading. We obtained a near linear response when the pH of water was in the range 5−9.

Generally calibration of moisture sensor was done by 1) weight and 2) volume methods, however these suffer from inconsistent results due to variation of soil density, evaporation, and porosity of different soils and so on. Therefore, we used the following equation to calibrate the sensor. Moisture (%) = $(\text{Max(V)} - \text{Min(V)}/\text{Min(V)}) \times 100$. Max(V) is the voltage output of dry soil (1.0 V in Figure 4A), Min(V) is the voltage output for a given moisture level. For e.g., when the output voltage is 0.673 V, then from formula % moisture is 48.6%.

■ RESULTS AND DISCUSSION

The architectural components and the complete architect of the sensor are shown in Figure 1A and B. The proposed moisture sensor consisted of an Al anode with a highly negative standard reduction potential ($E° = −1.66$ V vs SHE) and a polyaniline (PANI) conducting polymer coated on one side of the Whatman 40 filter paper (with a formal potential of 0.3 V vs SHE; see the explanation of Figure 2D) as the cathode
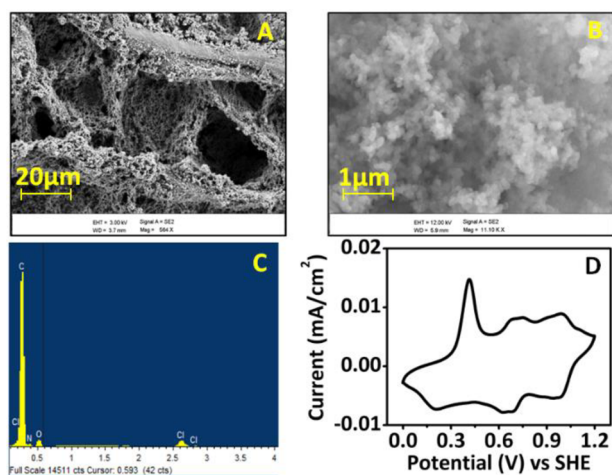

Figure 2. SEM images of PANI ES form coated on Whatman filter paper (A) at low magnification and (B) at high magnification. (C) EDX spectrum of PANI ES. (D) Cyclic voltammogram of a PANI coated glassy carbon electrode in 0.1 M H_2SO_4 at a scan rate of 50 mV/s.

electrode.[16] The PANI electrode was fabricated in such a way that the coated side was wrapped around a Teflon rod with the paper side facing the soil (see the Experimental Procedures for details). This is expected to protect the PANI surface from aberrations and scratches while allowing the communication to the soil through the voids and pores present in the paper, as observed in the scanning electron microscopy (SEM) images

(Figure 2A and B). Conducting PANI was coated on the paper by oxidative polymerization as described in the Experimental Procedures.

Polyaniline showed interlinked and nearly spherical polymeric particles with individual diameter of ∼100−200 nm (Figure 2A and B). Energy dispersive spectroscopy (EDS), Figure 2C, clearly demonstrated the presence of C and N along with Cl dopant, unambiguously revealing that as synthesized polymer was in the conducting state (ES), which was further confirmed by the UV−vis spectroscopy analysis described below (Figures 3B and 5 and 6). In the cyclic voltammogram of
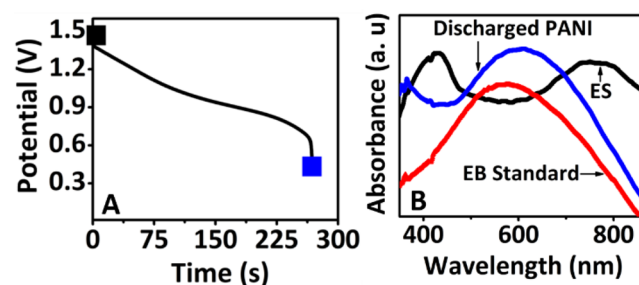

Figure 3. (A) Galvanostatic discharge curve for an Al-PANI battery in 0.1 M H_2SO_4 at a rate of 500 μA. (B) UV−vis spectrum of a PANI electrode before and after discharge along with the PANI EB standard.

PANI in 0.1 M H_2SO_4, Figure 2D, the well-defined redox transformation of PANI into conducting emeraldine salt (ES) and the nonconducting emeraldine base (EB) can be seen with a formal potential of 0.3 V, and the nature of the votammetric profile is in line with the literature data.[16] It is well-known that this fast redox transformation occurs with synchronized anion transfer, thereby providing pseudocapacitive characteristics to the PANI electrode.[17−19]

Since the formal potential of the PANI redox couple was 0.3 V vs SHE, when it was coupled to an Al electrode with a negative standard reduction potential of −1.66 V (vs SHE), a Galvanic cell with a theoretical OCV of 1.96 V was expected. Indeed, when an Al electrode was coupled to a PANI electrode in H_2SO_4, the resulting Galvanic cell demonstrated an OCV of ∼1.5 V with a well-defined discharge plateau around 1 V (Figure 3A). The drastic voltage drop observed close to 0.5 V (at ∼260 s) in the discharge curve indicated the completion of the discharge process. Overall, the demonstrated behavior is typical for many energy storage and conversion devices.[20−22] A lower OCV value from the expected 1.96 V could be due to the electrolyte resistance, Al oxide formation, etc. UV−vis spectroscopy furnishes particulars about the π electron conjugation along the polymeric backbone in both conducting ES and nonconducting EB forms. The UV−vis spectrum of the EB standard (Figure 3B (red trace)) showed an absorption band at 570 nm referable to the π−π* transition of an electron from the HOMO of the benzenoid structure to the LUMO of the quinoid structure.[23−26] PANI before discharge (black trace, Figure 3B) showed two absorption bands at 430 and 752 nm due to polaron band transitions and is typical of conducting PANI, ES form.[27,28] The UV−vis spectrum of the PANI electrode before and after discharge (black and blue traces, Figure 3B) demonstrated that the spectral pattern after discharge is now identical to the EB standard, unambiguously confirming the conversion of ES to EB during the discharge process. Based on this, the following half-cell reactions (eqs 1 and 2) are suggested, and the discharge chemistry is dominated

by the dedoping of PANI ES form to EB form with the simultaneous oxidation of Al. The discharge plateau was dominated by PANI, as the Al anode is in large excess and the voltage gradually dropped in the plateau region and almost rapidly when the EB formation was completed (Figures 2D and 3).

At Anode:

$$Al \rightarrow Al^{3+} + 3e^- \tag{1}$$

At Cathode:

$$ES + e^- \rightarrow EB + Dopant \tag{2}$$

We exploited this Galvanic cell for designing a moisture sensor for soil analysis. The working principle is as follows. When a Galvanic cell consisting of an Al-PANI system is inserted into the soil, the OCV it develops is heavily dependent on the amount of moisture present, as dry soil as a whole is ionically insulating. In the presence of moisture, as the PANI is in a heavily doped state, given the pH of water is above the pK_a of PANI,[29] it may undergo spontaneous dedoping reaction with a resulting voltage shift. As the OCV of the Al-PANI system is dependent on the extent of this dedoping process (as shown in Figure 3A) which in turn is dependent on the moisture levels present in the soil, it can be exploited to design a soil moisture sensor.

The Al-PANI system in dry soil delivered an average open circuit voltage of 1.0 V. The decreased OCV from the theoretically expected value and the one obtained in Figure 3A may be due to the infinite resistance the probes experience in dry soil. Since the proposed sensor is potentiometric in nature, it is very important to maximize the output voltage, as it will significantly improve the detection limit and sensitivity. Potentiometric sensors so far failed to make a breakthrough in soil moisture analysis because conventional reference electrodes are very delicate and can provide only a marginal voltage to the total potential difference and their sole presence is to provide a stable reference voltage, which is impossible given the infinite soil resistance. In such sensors, given the fact that, in the soil, ionic conductance is very much obstructed, the majority of the developed potential difference will be lost due to huge IR loss. However, in the case of Al-PANI, the two electrode system, given the very high theoretical voltage of 1.96 V, it is expected to provide a reasonable voltage difference (in the present case, 1.0 V) between the two electrodes when immersed in the soil, justifying the architecture of a two electrode Galvanic cell type configuration for soil moisture sensing.

The OCV dropped and stabilized for every increment in moisture content, as seen from the voltage vs moisture profile (Figure 4A), and it should be seen in the context of Figure 3A that it was observed that it took almost 5–10 min to stabilize the voltage after each moisture addition. The calibration plot (Figure 4B) demonstrated a near linear response (each calibration point is an average of 3 different measurements), the sensitivity calculated (based on a linear fit function) was 5.13 mV/% moisture, and the possible detection limit obtained by assuming a signal-to-noise ratio of 3 was 0.12%, presenting a decent sensor response.

To prove that PANI dedoping (or discharge) in the presence of moisture is responsible for the voltage shift, we carried out several analyses by different techniques. UV–vis spectral analysis of PANI before and after usage (for moisture analysis as shown in Figure 4) is shown in Figure 5A, and the spectral
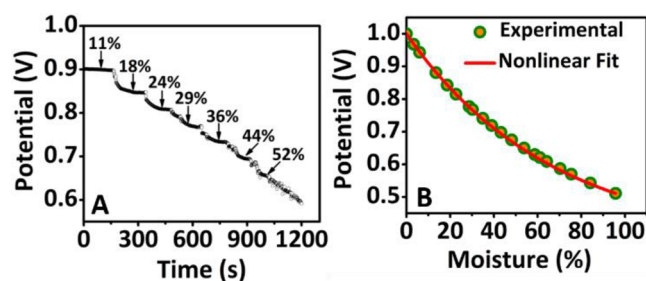

Figure 4. (A) Voltage vs time profile of the Al-PANI Galvanic cell type sensor for different moisture levels in the soil. (B) Calibration plot for different moisture levels in the soil.
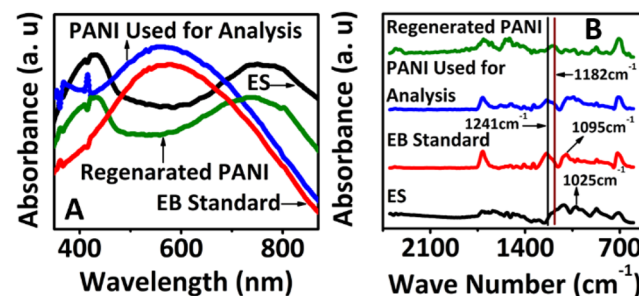

Figure 5. Characterization of a PANI electrode before and after soil moisture sensing: (A) UV−vis spectra and (B) FTIR spectra.

pattern after usage (blue trace) is now identical to the EB standard (red trace), confirming the transition of the ES to EB form during the moisture analysis. Therefore, the chemistry during moisture analysis is coherent to the Galvanic cell discharge chemistry shown in Figure 3A and B. Quite interestingly after the used PANI was kept in 1 M HCl for a few minutes, it can be seen that the PANI ES form was regenerated (Figure 5A, green trace). This is an important observation because it proves that the designed sensor is regenerable by a simple process and hence can be repeatedly used as explained below.

The identicalness of the chemistry of the Galvanic cell to that during soil moisture sensing was further supported by FTIR, XRD, and XPS analyses. In the FTIR spectra (Figure 5B), the characteristic peaks at 1241 and 1095 cm^{-1} for EB standard[30−33] were shifted in the protonated ES form (as marked). The peaks at 1182 and 1025 cm^{-1} were due to the ES form and were derived from the protonated $-NH^+$ vibrations, which were seen to be not prominent in the EB form.[34] The IR spectral patterns were largely identical for the used PANI and EB standard, and the spectral patterns of the ES form became, to some extent, identical to the regenerated PANI. These are in line with UV−vis spectral data and suggest that the sensing chemistry is identical to Galvanic cell discharge chemistry and that the sensor is regenerable and reusable. However, as widely reported in the literature, the FTIR of the EB and ES forms exhibited only marginal differences, and hence, we sought into other characterization techniques such as XRD and XPS.

The diffraction patterns of the ES and EB standards (Figure S3 (Supporting Information)) were essentially identical, except for some degree of broadening in the case of EB, since the ES form is more crystalline than the EB form.[35,36] From the full width at half-maximum (fwhm), it can be said that the fwhm for the used PANI was higher compared to the ES form and it decreased after treating with 1 M HCl. A closer look shows that

the diffraction pattern at $2\theta = 23.1°$ was slightly downshifted in the case of used PANI, similar to the EB form, and after treatment with HCl, it became upshifted, similar to the ES form (Figure S3B). The absence of a protonated N signal (in the range 400−403 eV) in the deconvoluted N (1S) XPS signal (Figure 6) for the used PANI and its reappearance in the HCl
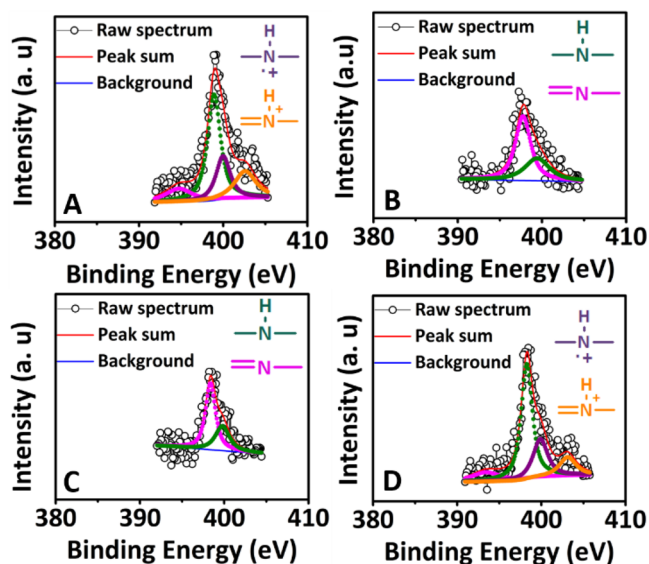

Figure 6. N(1s) XPS spectra of (A) PANI ES form, (B) EB standard, (C) PANI used for analysis, and (D) used PANI after regeneration.

treated PANI[37,38] supported that the ES form was moisture sensitive, and its conversion to the EB form was responsible for the sensor readout and the sensor was regenerable by simply treating it with 1 M HCl. Therefore, the sensor we developed is quickly regenerable and the chemistry occurring at the cathode during soil moisture analysis is identical to the Galvanic cell discharge chemistry. It should be noted that though the final outcome of soil moisture sensing at Al-PANI electrodes as a whole is identical to the end product in the Galvanic cell discharge chemistry as shown in Figures 3B and 4−6, the actual sensing mechanism is not the result of a direct discharge chemistry as shown in eq 2, as the outflow of electrons from Al is impeded by the voltmeter. Since the pK_a of PANI is 4.75[29] and the pH of added water is 7, the former undergoes a spontaneous dedoping from the ES to EB form (eq 3) and the resulting voltage shift is referenced versus an Al electrode having high negative standard reduction potentials. Therefore, in the presence of soil moisture, the total voltage between Al-PANI probes decreases, which is identical to the Galvanic cell during the discharge chemistry (Figure 3A), and the end products of Galvanic cell discharge chemistry are coherent to 100% moisture levels (Figures 3B and 5 and 6). Further, the complex impedance plot at Al-PANI sensing probes during moisture sensing (see the discussion in Figure 8) unambiguously confirms the occurrence of charge transfer at the sensing electrode(s)−moisture interface. Taken together, it can be said that the designed sensor is a Galvanic cell type soil moisture sensor. The total voltage at Al-PANI electrodes reached a minimum value close to 0.5 V at 100% moisture levels (Figure 4), and further addition of water did not significantly alter the voltage levels thereafter. This should be read in the context of Figure 3A, where a drastic voltage drop was observed close to 0.5 V, indicating the completion of the discharge process.

Therefore, the saturation voltage at 0.5 V was taken as the point at which the sensor requires a regeneration for multiple soil moisture analysis.

The multiple analysis carried out using the same Al-PANI system is shown in Figure 7. It is of note that the sensor was
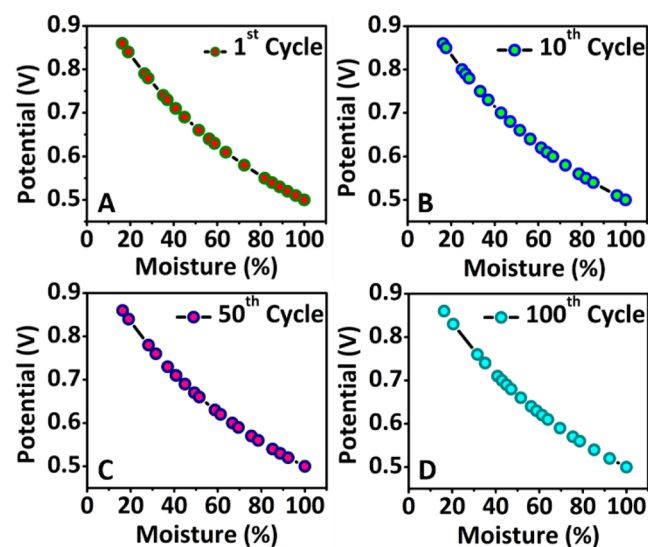

Figure 7. Cycling performance of an Al-PANI moisture sensor for (A) 1st cycle, (B) 10th cycle, (C) 50th cycle, and (D) 100th cycle. After each cycle the PANI electrode was regenerated by treating with 1 M HCl.

regenerated after every cycles by treating with 1 M HCl. The sensor delivered a decent response with a reasonably stable voltage response for similar moisture levels over 100 cycles. In an attempt to check the reproducibility of the sensor, different moisture levels were analyzed over 100 cycles using the same Al-PANI system, and the sensor output is presented in Figure S4. A stable and coherent sensor readout can be seen over cycling for the entire soil moisture levels, evidencing the utility of the architecture in real applications.

We have fabricated a moisture sensing device based on this Al-PANI system. The block diagram for the total device is presented in Figure S2A, and the first block is the sensor (see Experimental Procedures for more details). The electronic circuitry is shown in Figure S2B. The overall picture of the sensing device is shown in Figure 1B, where the output of the sensor is given to the microcontroller and displayed in the alphanumeric liquid crystal display. The accompanying video (Video 1, Supporting Information) shows that in the presence of moisture the voltage dropped and then stabilized and when the soil was dried; the sensor demonstrated the tendency to recover, confirming a near linear sensor response. Further we have fabricated an indicator type soil moisture sensor which can signal to the end user when the soil moisture levels go below critically low levels. This will help the end user in maintaining the optimum soil moisture levels at times when effective water management practices are required. This is expected to prevent water starvation/flooding of plant roots, thereby averting crop damage apart from helping toward effective irrigation strategies. The accompanying video (Video 2, Supporting Information) demonstrates that when the soil moisture level goes below 10% the sensor activates the red light emitting diode (LED) and above this the green LED is activated, thereby serving as a

smart sensor which can communicate directly with the end user.

$$ES \xrightarrow{H_2O(pH=7)} EB + Cl^- \qquad (3)$$

In order to prove that charge transfer during the dedoping at the interface of PANI in the presence of soil moisture is responsible for the sensor readout voltage, electrochemical impedance spectroscopy was carried out (Figure 8). As the
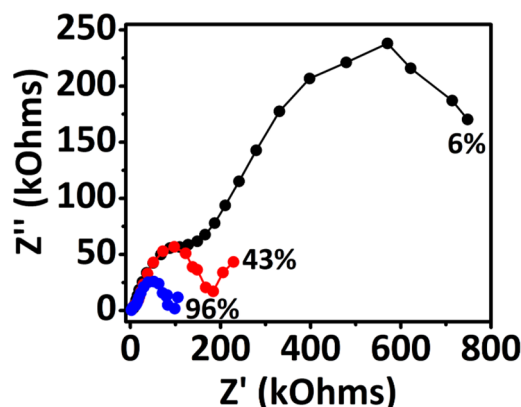

Figure 8. Electrochemical impedance spectra of Al-APNI sensing electrodes during soil moisture sensing. The spectra were acquired at 0 V vs OCV in the frequency range 100 kHz to 10 mHz.

semicircle has contributions from both the interfaces, it was not possible to separate the individual contributions. Since the diameter of the semicircle observed in the complex impedance plot (Nyquist) is directly proportional to the charge transfer resistance, it can be said that charge transfer at the Galvanic cell electrodes drastically decreased with the moisture levels, unambiguously confirming that the charge transfer at the electrode/moisture interface was responsible for the sensor response and is evidently identical to the discharge chemistry occurring in the Galvanic cell.

CONCLUSIONS

We have successfully fabricated the first Galvanic cell type sensor for soil moisture analysis by exploiting the redox energies of Al and polyaniline electrodes. The designed sensor is simple, inexpensive, and portable and hence can be used for on-site field analysis to get the spatial and temporal variations of soil moisture in an area. The projected sensor response is probe size independent, unlike the state of the art moisture sensors and hence can provide a sustainable sensor readout under the strongly aberration conditions commonly encountered in soil moisture analysis. The sensor mechanism is proved to be a typical Galvanic cell type discharge reaction by a range techniques such as UV−vis spectroscopy, FTIR, XRD, and XPS analysis. Electrochemical impedance spectroscopy unambiguously confirmed that charge transfer at the interface of sensing electrodes is responsible for the sensor readout. The fabricated sensor is regenerable by treating with 1 M HCl and hence can be used for multiple analysis with little readout hysteresis. Further we have fabricated an indicator type smart soil moisture sensor which can signal to the end user when the moisture levels go below critically low levels, thereby averting crop damage apart from assisting effective and efficient agricultural strategies. We hope that our findings will be beneficial for developing effective and energy efficient irrigation strategies,

understanding the heat and water transfer at the atmosphere−land interface, forecasting the risk of natural calamities, and so on.

ASSOCIATED CONTENT

Ⓢ Supporting Information

Image of PANI coated filter paper, XRD pattern, block diagram with complete electronic circuitry, and reproducibility test for the sensing device. The Supporting Information is available free of charge on the ACS Publications website at DOI: 10.1021/acs.analchem.5b01653.

AUTHOR INFORMATION

Corresponding Author

*E-mail: musthafa@iiserpune.ac.in. Tel: +91(020)25908261.

Notes

The authors declare no competing financial interest.

ACKNOWLEDGMENTS

REFERENCES

(1) Mittelbach, H.; Lehner, I.; Seneviratne, S. I. *J. Hydrol.* **2012**, *430−431*, 39−49.

(2) Zehe, E. *Hydrol. Earth Syst. Sci. Discuss.* **2010**, *6*, C3145−C3151.

(3) Bircher, S.; Skou, N.; Jensen, K. H.; Walker, J. P.; Rasmussen, L. *Hydrol. Earth Syst. Sci. Discuss.* **2011**, *8*, 9961−10006.

(4) Robinson, D. A.; Campbell, C. S.; Hopmans, J. W.; Hornbuckle, B. K.; Jones, S. B.; Knight, R.; Ogden, F.; Selker, J.; Wendroth, O. *J. Vadosezone* **2008**, *7*, 358−389.

(5) Tyson, E. O.; Michael, H. C.; Richard, H. C.; Wouter, A. D.; Clara, S. D.; Yutaka, H.; Yann, H. K.; Eni, G. N.; Eric, E. S.; Marek, Z. *Soil. Sci. Soc. Am. J.* **2013**, *77*, 1888−1919.

(6) Batlle, B. L.; Vanden, H. B. J.; Strengers, B. J.; Minnen, J. G. *J. Earth. Sci. Clim. Change* **2014**, *5*, 1−11.

(7) Roger, A.; Pielke, S.; Roni, A.; Michel, R.; Johannes, D. A.; Xubin, Z.; Scott, D. A. *J. Global Change Biol.* **1998**, *4*, 461−475.

(8) Lim, Y.; Hong, J.; Lee, T. *J. Meteorol. Atmos. Phys.* **2012**, *118*, 151−161.

(9) Pariva, D.; Ashi, Q.; Ruchi, B.; Syed, A. H. *J. Hydrol.* **2012**, *458−459*, 110−117.

(10) Topp, G. C.; Davis, J. L.; Bailey, W. C.; Zebchuk, W. D. *Can. J. Soil. Sci.* **1984**, *642*, 313−321.

(11) Reynolds, S. G. *J. Hydrol.* **1970**, *11*, 258−273.

(12) Chanasyk, D. S.; Naeth, M. A. *Can. J. Soil. Sci.* **1996**, *76*, 317−323.

(13) Wang, B. X.; Fang, Z. H.; Yu, W. P. *Int. J. Thermophysics* **1989**, *10*, 211−225.

(14) Markus, S.; Franz, K.; Rainer, S. *Sensors* **2009**, *9*, 2951−2967.

(15) Gohil, V. M.; Pabari, J. P.; Panchal, S. R.; Nayak, V. H. *J. Engineering* **2012**, *2*, 837−843.

(16) Li, M. H.; Wang, R. T.; Ten, C. W. *J. Power Sources* **2006**, *164*, 519−526.

(17) Lijia, P.; Hao, Q.; Chunmeng, D.; Yun, L.; Lin, P.; Jianbin, X.; Yi, Shi. *Int. J. Mol. Sci.* **2010**, *11*, 2636−2657.

(18) Katsuhiko, N.; Masayuki, M. *Electrochem. Soc. Interface* **2008**, *17*, 44−48.

(19) Ashok, K. S.; Jong, H. K.; Yong-Sung, L. *Int. J. Electrochem. Sci.* **2009**, *4*, 1560−1567.

(20) Meyer, M.; Cyril, V.; Lydie, V.; Mehdi, A.; Olivier, F. *J. Mater. Chem.* **2014**, *2*, 12162−12165.

(21) Dunst, A.; Epp, V.; Hanzu, I.; Freunberger, S. A.; Wilkening, M. *Energy Env. Sci.* **2014**, *7*, 2739−2752.

(22) Cheng, H.; Scott, K. *Appl. Catal. B: Env.* **2011**, *108−109*, 140−151.

(23) Dipak, D.; Tridib, K. S.; Devasish, C.; Arun, C. *J. Colloid Interface Sci.* **2005**, *283*, 153−159.

(24) Farahkamwal, A.; Thahir, J. *J. Chem. Soc. Pak.* **2007**, *29*, 553−557.

(25) Gizdavic, N. M.; Graham, A.; Bowmaker, G. *Polymer* **2008**, *49*, 3070−3075.

(26) Huang, W. S.; MacDiarmid, A. G. *Polymer* **1993**, *34*, 1833−1845.

(27) Sfez, R.; De, Z. L.; Turyan, I.; Mandler, D.; Yitzchaik, S. *Langmuir* **2001**, *17*, 2556.

(28) Stejskal, J.; Gilbert, R. G. *Pure Appl. Chem.* **2002**, *74*, 857.

(29) Hatchett, D. W.; Josowicz, M.; Janata, J. *J. Phys. Chem. B* **1999**, *103*, 10992−10998.

(30) Chakane, S.; Likhite, P.; Jain, S.; Bhoraskar, S. V. *Trans. SAEST* **2002**, *37*, 35.

(31) Hussain, A. M. P.; Kumar, B. A. *J. Appl. Polym. Sci.* **1999**, *71*, 2169.

(32) Seon, J. K.; Su, R. S.; Geoffrey, M. S.; In, Y. K.; Sun, I. K. *J. Appl. Polym. Sci.* **2005**, *96*, 867−873.

(33) Chen, S. A.; Lee, H. T. *J. Macromol.* **1995**, *28*, 2858−2866.

(34) Gomes, E. C.; Oliveira, M. A. S. *Am. J. Polym. Sci.* **2012**, *2*, 5−13.

(35) Sudha; Devendra, K. *Der. Chem. Sinica.* **2013**, *4*, 60−66.

(36) Pouget, J. P. *Macromolecules* **1991**, *24*, 79−789.

(37) Yue, J.; Epstein, A. J. *Macromolecules* **1991**, *24*, 4441−4445.

(38) Mu, Y. H.; Chun, J. C.; Hsiao, C. C.; Rung, Y. T.; Wen, C.; Chun, L. C.; Yin, C. L. *Sensors* **2011**, *11*, 5873−5885.